J. Dairy Sci. 101:1–9
https://doi.org/10.3168/jds.2018-14749

Technical note: Fourier transform infrared spectral analysis in tandem with ^{31}P nuclear magnetic resonance spectroscopy elaborates detailed insights into phosphate partitioning during skimmed milk microfiltration and diafiltration

Mattia Boiani,*† Richard J. FitzGerald,† and Phil M. Kelly*[1]
*Teagasc Food Research Centre, Moorepark, Fermoy, Co. Cork, Ireland, P61 C996
†Department of Biological Sciences, University of Limerick, Castletroy, Limerick, Ireland, V94 T9PX

ABSTRACT

Our previous study identified peaks in the ^{31}P nuclear magnetic resonance (^{31}P NMR) spectra of skim milk, denoting the interaction of different phosphate species such as inorganic and casein-associated phosphate during the separation of colloidal and serum phases of skim milk by microfiltration (MF) and diafiltration (DF). In the current study, we investigated the same samples generated by the aforementioned separation using attenuated total reflectance (ATR) Fourier transform infrared (FTIR) spectroscopy analysis. The results confirmed that the technique was not only capable of differentiating between the mineral equilibrium of the casein phosphate nanocluster (CPN) and milk serum, but also complemented the application of ^{31}P NMR. An ATR-FTIR broad band in the region of 1,055 to 1,036 cm^{-1} and a specific band at 1,076 cm^{-1} were identified as sensitive to the repartitioning of different phosphate species in milk in accordance with the ^{31}P NMR signals representing casein-associated phosphate and inorganic phosphate in the serum. A third ATR-FTIR signal at 1,034 cm^{-1} in milk, representing precipitated inorganic calcium phosphate, had not previously been detected by ^{31}P NMR. Thus, the results indicate that a combination of ATR-FTIR and ^{31}P NMR spectroscopies may be optimally used to follow mineral and protein phase changes in milk during membrane processing.
Key words: Fourier transform infrared, casein, phosphate nanocluster, micellar structure

Technical Note

Casein is the principal protein component of milk consisting of 4 individual phosphoproteins: α_{S1}-CN, α_{S2}-CN, β-CN, and κ-CN, which are self-assembled as a casein micelle (**CM**; Fox and Brodkorb, 2008). Casein micelles of milk have been studied over several decades (Horne, 2006; De Kruif, 2014) by researchers who have been fascinated by such a complex and unique conformation. However, caseins' lack of conventional secondary structure (Holt, 1992) makes it particularly challenging to characterize. Innovation in membrane-based separation technology in recent decades has made it possible to selectively isolate casein in its micellar form (CM) from skim milk, thus presenting researchers an opportunity to probe the interrelationship between the colloidal state of casein and its surrounding serum phase using advanced analytical techniques. A structural role that calcium phosphate plays at the core of CM is its contribution to the formation of casein phosphate nanocluster (**CPN**; Lenton et al., 2015). The CPN is primarily responsible for a key aspect of milk's nutritional value through its capacity to maintain the stability of a saturated solution of phosphate and calcium (Gaucheron, 2005) without precipitation and sedimentation of calcium phosphate salt from milk. In our previous study (Boiani et al., 2017), we found that by monitoring the various states of soluble and colloidal phosphate using ^{31}P nuclear magnetic resonance (**NMR**) during microfiltration (**MF**) and diafiltration (**DF**), instances of casein solubilization and loss of CPN structure could be identified during these separation processes. Thus, it is evident that such phase separation disturbs the equilibria occurring between CM-containing CPN and milk serum–containing inorganic orthophosphate (Holt et al., 1996; Lenton et al., 2015). Various investigations have been done in the recent past on CPN structure; such studies include the elaboration of a thermodynamic equilibrium model for the sequestration of calcium phosphate by casein micelles (Holt, 2004; Little and Holt, 2004; Mekmene et al., 2009) and the exploration of cluster formation by phosphopeptides generated by casein hydrolysis (Holt et al., 1996; Cross et al., 2005;

Received March 14, 2018.
Accepted July 10, 2018.
[1]Corresponding author: phil.kelly@teagasc.ie

Lenton et al., 2016). These studies suggest that CPN structure is composed of an amorphous calcium phosphate (**ACP**). Such a structure represents a low-order conformation that makes its investigation difficult, and it is usually considered to be an unstable precursor of hydroxyapatite, another calcium phosphate salt structure. However, it has been shown that CM is able to stabilize ACP within it (Holt et al., 1996, 1998; Cross et al., 2005; Lenton et al., 2015). In addition, CPN may be subject to perturbation because it can be influenced by the ionic environment in which CM is suspended (Boiani et al., 2017). From an analytical perspective, this makes sample preparation extremely challenging, especially when attempting to obtain a representative CPN of CM (Holt et al., 2003). In particular, calcium, phosphate, organic acid, and casein proteins are all involved in nanocluster formation (Holt, 2004). Considering the constraints surrounding sample preparation for the investigation of the milk mineral behavior, attenuated total reflectance (**ATR**) Fourier transform infrared spectroscopy (**FTIR**) was considered an accessible spectroscopy technique that does not require sample modification. It has been already used to examine some features of milk and dairy products; for example, the secondary structure of casein (Byler and Farrell, 1989; Curley et al., 1998), the influence of UHT processing on different milk components (Grewal et al., 2017), and the calcium phosphate binding ability of cheese (Upreti and Metzger, 2006). Fourier transform infrared spectroscopy was also used to investigate inorganic calcium phosphate material (Trpkovska et al., 1999; Berzina-Cimdina and Borodajenko, 2012; Hirsch et al., 2014) alone or in combination with casein phosphopeptides (Lenton et al., 2016). Thus, we set out to apply ATR-FTIR to characterize the main forms of phosphorus present in milk with a view to distinguishing between CPN and inorganic phosphate ($\mathbf{P}_i$). Three different ions (orthophosphate, calcium, and citrate) simulating those known to be bound to the phosphate nanocluster (Gaucheron, 2005) were incorporated into DF solutions used to wash CM during MF at the laboratory scale. This approach complements and extends our previous work using ^{31}P NMR specifically to investigate CPN (Boiani et al., 2017). Thus, after establishing a baseline ATR-FTIR spectrum for CM produced by regular MF and DF, it was now possible to modify the DF step by incorporation of ions in DF solutions both individually and in the approximate combination that reflects their functional role in a typical soluble milk serum.

Solutions of acid orthophosphate (0.1 mol/L) were studied at different pH (6.0, 6.5, 7.0). Inorganic calcium phosphate ($\mathbf{CP}_i$) powder was prepared by mixing sodium orthophosphate bibasic and calcium chloride with a molarity ratio P:Ca = 1:3–2:3–3:3. During precipitation the pH of the solution was maintained at pH 7.0 with sodium hydroxide (0.1 *M*). The precipitate obtained was dried for 15 h at 65°C in a vacuum oven at −0.1 MPa, and immediately analyzed by ATR-FTIR.

A NovaSet-LS membrane (TangenX, Shrewsbury, MA) was used to microfilter (pore size 0.1 μm) pasteurized skimmed bovine milk at 40°C at constant feed pressure of 100 kPa. Six DF steps were performed, all based on an original starting volume of 1 L of milk. The DF process was initiated after concentrating the retentate to 500 mL and adding 500 mL of DF solution to restore the volume to 1 L. Thus, a total of 3 L of DF solution was used during the course of successive DF steps as previously described (Boiani et al., 2017). The individual solutions used for DF were (1) MilliQ water (Millipore; Purelab Flex 6, Elga LabWater, Lane End, UK; **DF-W**), (2) 20 m*M* sodium dibasic orthophosphate (**DF-P**), (3) 10 m*M* citric acid (**DF-Cit**), (4) 20 m*M* sodium dibasic orthophosphate + 10 m*M* calcium chloride [**DF-(P+Ca)**], (5) 10 m*M* citric acid + 10 m*M* calcium chloride [**DF-(Cit+Ca)**], and (6) 20 m*M* sodium dibasic orthophosphate + 10 m*M* citric acid + 10 m*M* calcium chloride [**DF-(P+Cit+Ca)**]. The individual or collective minerals included in the DF solutions (2) to (6) were chosen to minimize depletion of those specific minerals from milk that typically occurs during the DF process. Calcium and citrate (**Cit**) were added to the respective DF solutions at a level corresponding to their soluble content in milk (Gaucheron, 2005). Addition of P at 20 m*M* corresponded to the typical concentration of inorganic P in milk. All mineral solutions were adjusted to pH 7 using 0.1 *M* sodium hydroxide to control the influence of pH during the DF process. Samples were collected at the beginning of the process (skim milk sample) and at the end of DF [DF-W, DF-P, DF-Cit, DF-(P+Ca), DF-(Cit+Ca), and DF-(P+Cit+Ca)]. Sodium azide (0.3 mg/mL) was added to all samples to control microbial growth during refrigeration at 4°C. Two solutions of DF-(P+Ca) and DF-(P+Cit+Ca) were used to avoid precipitation of the insoluble calcium phosphate salt before the DF steps. Each DF step in those 2 cases was executed by first adding 250 mL of 40 m*M* P and then immediately adding 250 mL of 20 m*M* Ca or 20 m*M* Ca+Cit. This was performed to avoid calcium-casein aggregation, which is not reversible following the addition of P (Thomar et al., 2016).

Total Ca and P analyses were conducted by an external laboratory (Eurofins, Eurofins Cork Limited, Glanmire, Ireland) using atomic absorption (FT013) for determination of total Ca content and a colorimetric method (FT014) for total phosphorus content.

The mineral analysis used the following methods: Ca: AOAC 986.08, and P: AOAC 986.24 (AOAC, 1990).

The pH of milk and the final retentate was determined using a Mettler Toledo pH meter (Mettler-Toledo Ltd., Beaumont Leys, Leicester, UK). The pH meter was calibrated with standard pH solutions. The pH of skim milk and retentates was measured directly during the MF process at 40°C.

Evaluation of CM size was estimated using a Nano-ZS, (Malvern Zetasizer UK, Malvern, UK). Samples were diluted 1:100 using permeate solution obtained during the DF process to minimize multiple scattering effects. Measurements were performed in triplicate at 25°C. Results were calculated as cumulative mean diameter and referred to as hydrodynamic diameter (nm).

The FTIR spectra were generated within 1 to 3 d after preparation of all final retentates. The FTIR spectrometer used for this analysis was a 27 Tensor FTIR (Bruker UK Ltd., Coventry, UK) equipped with an attenuated total refraction BioATRCell II probe (Bruker UK Ltd., Coventry, UK) with a germanium crystal for liquid samples or a Pike MIRacle (Pike Technologies, Great Dunmow, Ireland) with a diamond crystal for solid samples. The acquisition temperature was kept constant using a Haake DC30-K20 Digital Control Bath (Thermo Scientific, Hemel Hempstead, UK). All liquid sample spectra were collected by subtracting the deionized water signal from the spectra with the exception of the skim milk sample, where permeate sampled during first-stage MF was used as background during FTIR analyses. The samples were equilibrated at 25°C and spectra collected between 4,000 cm^{-1} and 900 cm^{-1} with an instrument resolution of 4 cm^{-1}. Spectra were obtained from 400 scans of each sample. Further manipulation of the spectra took into consideration the contribution of atmosphere and water, vector normalization on account of the protein signal, specifically with bands belonging to amide I and II (1,800–1,350 cm^{-1}), and deconvolution with a lorentzian equation between 1,300 cm^{-1} and 900 cm^{-1} using the manual deconvolution program (bandwidth 19.9 and noise reduction 0.29). All spectra manipulations were conducted using Opus 5.5 (Bruker Optik GmbH, Ettlingen, Germany) software.

All samples referred to in the 31P NMR study (Boiani et al., 2017) and their associated analytical data (pH, TS, Ca, and P) were used during the current FTIR investigations. Analysis of variance was undertaken using Minitab version 17 (Minitab Inc., State College, PA). The level of significance was established at $P < 0.05$. Fisher's multiple-comparison test was used for paired comparison of treatment means and the level of significance was determined at $P < 0.05$.

When addressing the equilibrium state of phosphate in milk, only 2 types matter: phosphate in serum solution (i.e., P_i) and phosphate bonded with calcium within the CPN. The presence in milk of phosphorus can be beneficially studied using FTIR. From the outset of the study, it was necessary to generate profiles of FTIR spectra for the phosphate compounds of interest. The P_i in serum corresponds to a solution of orthophosphate at a typical milk pH of 6.8. The P_i FTIR spectra obtained at various pH values are depicted in Figure 1a. We decided to focus our investigation in the region between 1,200 and 950 cm^{-1} of the milk spectrum. The greater part of an FTIR milk spectrum (Figure 2a) is dominated by protein and organic molecule signals, whereas the area of interest (1,200–950 cm^{-1}) is mainly associated with minerals and milk carbohydrate (Grewal et al., 2017). With reference to phosphorus, this area is associated with the P–O stretch (Hirsch et al., 2014). We speculate that binding of Ca^{2+} and formation of CPN influence the energy bond between phosphate and oxygen and, consequently, its stretching energy, resulting in the generation of different spectra between P_i and CPN. We detected no change in band wavenumber for the P_i spectra obtained at different pH values (Figure 1a). Three bands were found, 2 of low intensity present at 1,157 cm^{-1} and 989 cm^{-1} and 1 high-intensity band at 1,076 cm^{-1}. Although the absorbance of these bands differed with pH, this did not affect the primary qualitative outcomes of this study or, therefore, our final conclusions. The laboratory-prepared inorganic calcium phosphate (CP_i) used to simulate CPN was obtained, for simplicity, by precipitation of a solution of phosphate and calcium at pH 7 (as detailed in the description of inorganic sample preparation). Its spectrum was collected (Figure 1b and 1c) using the Pike probe for solid samples. Of the 6 main bands detectable in the full CP_i spectrum (Figure 1b), only 3 in the area of interest for this study (1,200–950 cm^{-1}; Figure 1c), specifically at 1,124, 1,053 and 983 cm^{-1}, and a single low-intensity band at 1,002 cm^{-1} were considered. As combinations of different molar ratios of calcium ions and phosphate used during the precipitation process did not influence the spectra of CP_i, we deemed it possible to adopt this spectrum as a reference for the putative occurrence of CPN spectra, even allowing for the possibility that different conformations between CP_i and CPN may lead to different FTIR spectra. However, in support of our hypothesis, the spectrum of CP_i characterized by our spectrophotometer (Figure 1b) was similar to that of dicalcium phosphate dihydrate ($CaHPO_4 \cdot H_2O$; Lenton

et al., 2016), which is considered the main calcium phosphate entity in the phosphate nanocluster.

A full skim milk spectrum, without any manipulation, is shown in Figure 2a. As already mentioned, the region between 1,200 and 950 cm^{-1} was considered appropriate for investigation of the relationship between phosphate and CPN, especially its higher intensity bands. However, additional compositional complexity occurs due to the overlap of milk carbohydrate (lactose) and fat signals (Zhou et al., 2006; Kher et al., 2007; Gebhardt

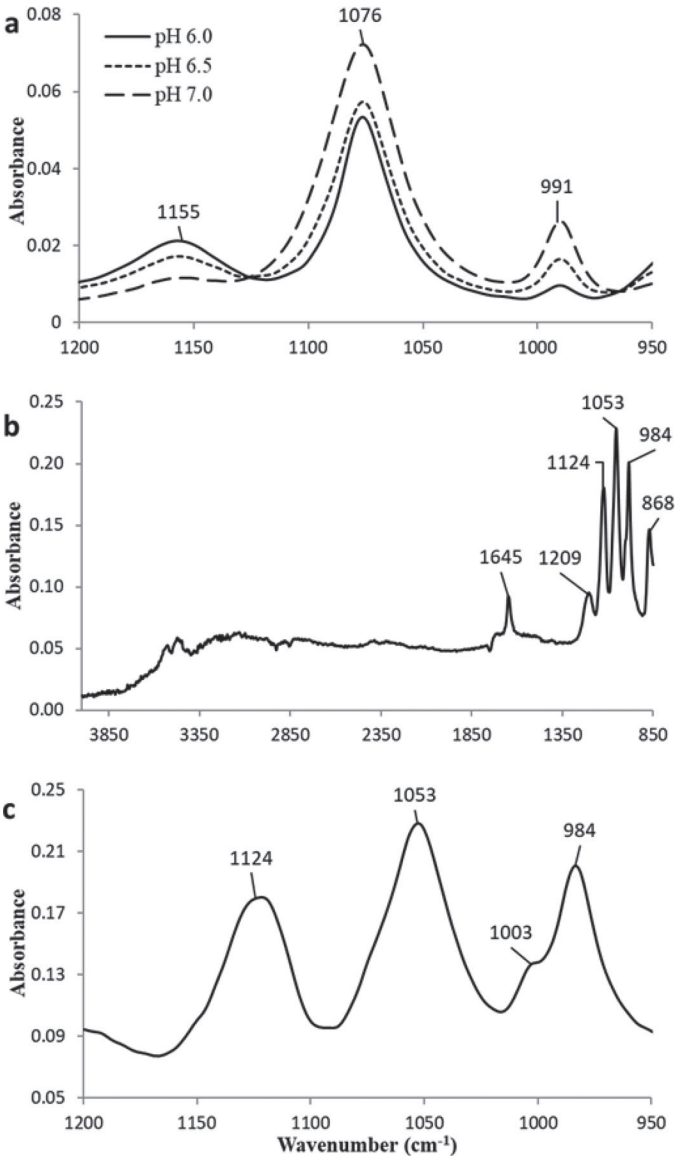

Figure 1. Fourier transform infrared (FTIR) spectra of (a) 10 m*M* orthophosphate solution (P_i) at different pH (6.0, 6.5, 7.0) obtained with liquid FTIR probe and (b and c) calcium phosphate precipitate (CP_i) at pH 7 obtained with solid FTIR probe: (b) full CP_i spectrum from 4,000 to 850 cm^{-1}, (c) expanded view of CP_i spectrum between 1,200 and 950 cm^{-1}.

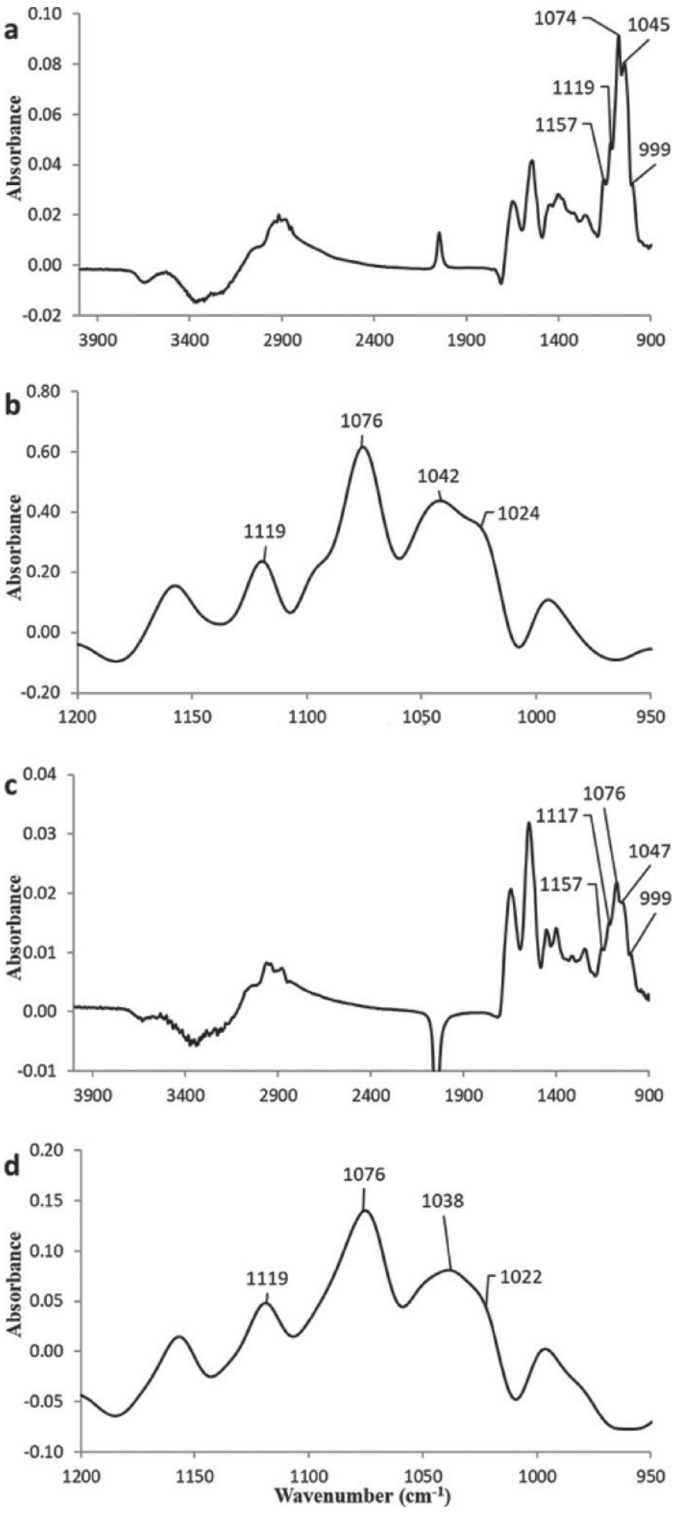

Figure 2. Fourier transform infrared (FTIR) spectra of skim milk using deionized water (a and b) and skim milk permeate (c and d) from 0.1-μm-membrane filtration as backgrounds: a and c refer to actual (unadjusted) full spectra of skim milk with deionized water and skim milk permeate backgrounds, respectively; b and d show the respective spectra of skim milk with deionized water and skim milk permeate backgrounds obtained following background correction, spectra normalization and deconvolution.

et al., 2011) with the mineral bands of interest in the spectra. Hence, fat interference was reduced by using skim milk (Figure 2a). The zone of higher intensity comprised a series of overlapping bands where a maximum was clearly recognizable. The higher intensity maxima are visible at 1,075 and 1,046 cm^{-1}, whereas several smaller peaks are evident at 1,154, 1,019, and 997 cm^{-1}. These latter values, even if close to the P_i and CP_i values, may be a sum of different signals of carbohydrate and minerals. After spectrum manipulation and deconvolution (Figure 2b), we could observe a main band at 1,076 cm^{-1} and 2 lower intensity bands at 1,157 and 990 cm^{-1} that could be associated with P_i in solution (Figure 1a), whereas the band at 1,119 cm^{-1} was similar to that representing CP_i (Figure 1c). In addition, we observed a broad band at 1,042 cm^{-1} with a shoulder at 1,024 cm^{-1} that, considering the absence of the band at 1,052 cm^{-1} of CP_i (Figure 1c), might be associated with displacement of the former. This band shifted slightly with respect to that identified in the initial analysis (Figure 1c). This difference between CP_i and CPN may be due to the aforementioned presence of lactose or other environmental factors where the 2 different components are found. To improve the quality of generated data, the spectra of skim milk were partially cancelled by using skim milk permeates generated by MF as background. In this way, we could subtract the signals from lactose and other soluble components present in skim milk serum. The resulting adjusted full spectrum (Figure 2c) shows the band already described with a reduced absorbance intensity and a band at 1,046 cm^{-1} that was reduced to a broad shoulder instead of the previous clear peak. The deconvoluted spectrum (Figure 2d) shows a small difference in the position of the bands with a slight shift of the broad band at 1,038 to 1,022 cm^{-1}, the intensity of which was similar to that of the band occurring at 1,119 cm^{-1} and, thus, generating a spectrum that more closely resembles that of CP_i (Figure 1b), although the CP_i band at 1,053 cm^{-1} is not visible.

With its selectivity for retention of primarily CM, MF in conjunction with DF readily permeates lactose, whey proteins, and the soluble salt phase of milk (Singh, 2007). The addition of different minerals during DF counters MF permeate losses and helps maintain specific ionic species in solution on both the retentate and permeate side of the membrane. Such inversions modify the mineral equilibrium of milk and allowed us to identify and associate FTIR signal response with specific species of phosphorus in the CM retentate. Figure 3a shows the full spectrum of DF-W before any ionic manipulation, in which the soluble phase (serum) has been permeated and removed. The spectrum of this sample (Figure 3a) is similar in shape to that of milk obtained with permeate as background (Figure 2c). However, some shifting of wavenumber is visible; for example, the maximum of the band visible at 1,076 cm^{-1} in Figure 2c has shifted at 1,090 cm^{-1} and the broad shoulder at 1,038 to 1,022 cm^{-1} has reduced intensity compared with that of the protein signals at 1,500 to 1,600 cm^{-1}. Figure 3b shows the FTIR spectra of the final retentate for DF-W after deconvolution. The high intensity band visible in skim milk at 1,038 to 1,022 cm^{-1} (Figure 2b and 2d) is no longer present. In its place is a low intensity band at 1,055 cm^{-1} corresponding to the same wavenumber of the band of CP_i that was visible in Figure 1c. Two bands belonging to soluble orthophosphate were shifted to higher wavenumber (1,082 and 996 cm^{-1} as opposed to 1,076 and 982 cm^{-1} in Figure 1a), whereas the band at 1,157 cm^{-1} remained unchanged. However, the calcium phosphate band (Figure 1c) was now broader (1,055–1,036 cm^{-1}) compared with that found in the same region (1,038–1,022 cm^{-1}) of the skim milk spectra (Figure 2d). Also visible on the spectrum (Figure 2d) were the shoulders (1,113 cm^{-1} and 982 cm^{-1}) associated with the bands at 1,082 cm^{-1}

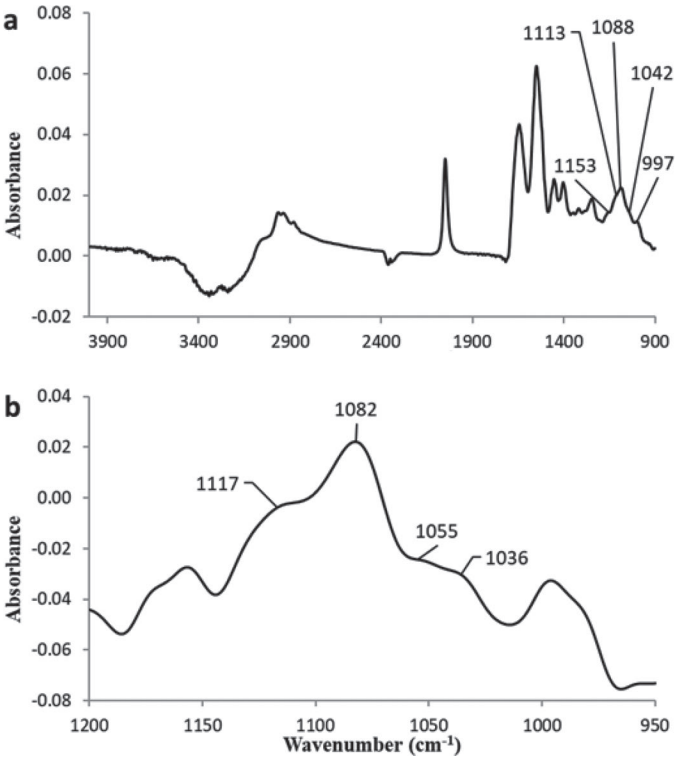

Figure 3. Fourier transform infrared (FTIR) spectra of the final retentate following with water diafiltration (DF-W): (a) retentate unadjusted full spectrum, (b) retentate spectrum following background correction, spectra normalization, and deconvolution.

and 996 cm^{-1}, respectively. These highlighted shoulders occur at the same positions in the spectrum as those identified for the calcium phosphate bands at 1,117 and 982 cm^{-1} in Figure 1c.

By adding P_i during the process of DF, it was possible to maintain the concentration of phosphate in the retentate and thus observe an increase in the P_i signal. Figure 4a shows the final retentates after DF-P and DF-P+Ca compared with DF-W. The DF-P spectrum showed an increase in all P_i band intensities (see Figure 1a). The CP_i bands were slightly increased; that is, more visible at 1,119 cm^{-1} with an increased intensity at the higher wavenumber of the broad band at 1,055 to 1,036 cm^{-1}. The DF-P+Ca treatment increased the concentration of calcium and phosphorus in the final retentate (Table 1), which contributed to an increased intensity of all P_i bands and the band at 1,119 cm^{-1} of the CP_i (see also Figure 1). The band at 1,055–1,036 cm^{-1} visible in DF-W and DF-P was not particularly evident, but a band at 1,034 cm^{-1} was prominent in this part of the spectra. Although the latter was not previously detected in the spectrum of CP_i (Figure 1b), it was evident in the spectra of skim milk (Figure 2) and DF-W (Figure 3) as part of the broader shoulder.

Chelating calcium from phosphate reduces the amount of cluster present in the CM. Citrate is a noted calcium chelating agent present in milk (Singh et al., 1991). Diafiltrating with citric acid should, therefore, reduce the calcium bound to CPN. Figure 4b shows the spectra obtained for DF-Cit and DF-Cit+Ca retentate samples compared with the retentate DF-W. The DF-Cit spectrum showed a decrease in intensity of the bands associated with CP_i, as previously expected, particularly the bands between 1,055 and 1,036 cm^{-1}. The bands belonging to the P_i spectrum did not show any relevant change. Diafiltration with Cit+Ca was performed to override the chelation of calcium by citrate and prevent solubilization of CPN. Therefore, as expected, the spectrum obtained was similar to DF-W in terms of absorbance and overall shape of the CP_i and P_i bands.

By maintaining the most influential ions for CPN equilibrium in the serum, we should be able to preserve the CPN present in the casein and reduce its loss during MF. The DF-P+Cit+Ca spectrum (Figure 4c) showed that all bands belonging to CP_i and P_i had increased intensity; for example, the band at 1,036 cm^{-1} was especially increased in intensity compared with DF-P.

An overall objective of this paper was to explore the use of ATR-FTIR to monitor shifts in the mineral equilibria in milk during MF and DF using the sampling regimen that we previously reported for ^{31}P NMR analysis (Boiani et al., 2017). As a first step, we decided to investigate the spectrum of singular inorganic phosphorus elements. The CP_i FTIR spectra identified in Figure 1b and 1c resemble those of brushite (Lenton et al., 2016), a calcium phosphate salt used as a biomaterial for dental repair and recognized as a precursor for formation of bones and teeth. In a further study,

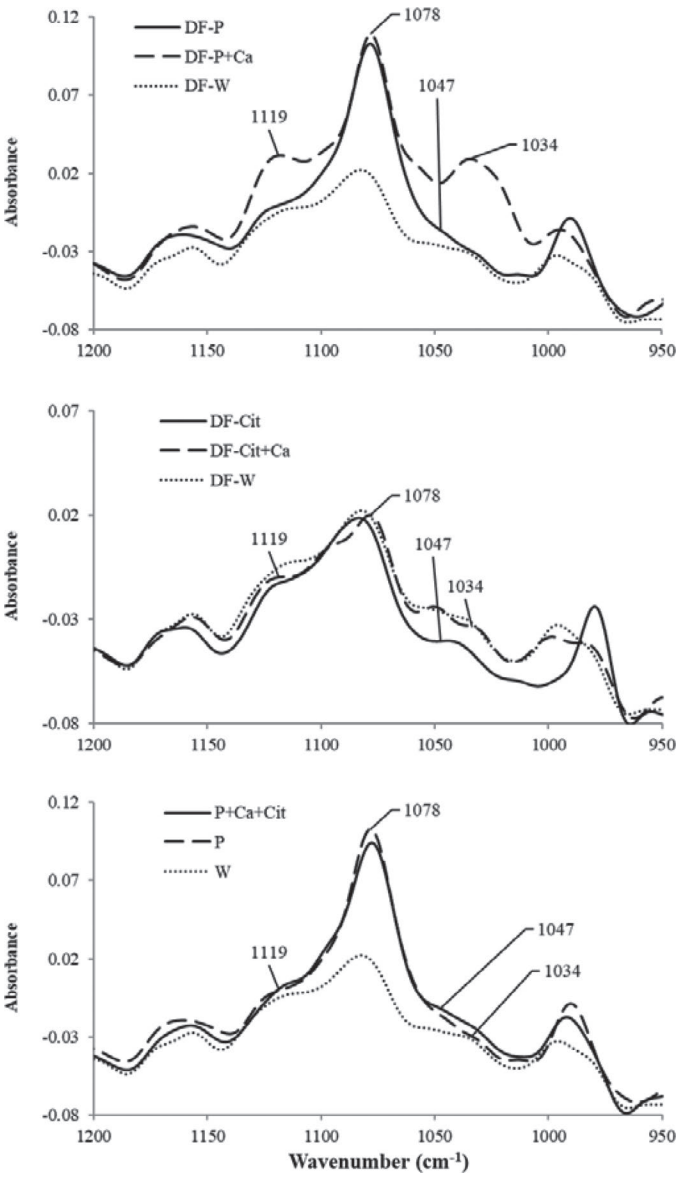

Figure 4. Fourier transform infrared (FTIR) spectra from final retentates following (a) diafiltration with phosphate (DF-P, solid line), diafiltration with phosphate plus calcium (DF-P+Ca, dashed line), and retentate following water diafiltration (DF-W, dotted line) shown as reference; (b) diafiltration with citrate (DF-Cit, solid line), diafiltration with citrate plus calcium (DF-Cit+Ca, dashed line), and retentate following water diafiltration (DF-W, dotted line) shown as reference; (c) phosphate plus calcium plus citrate diafiltration (P+Ca+Cit, solid line) and final retentates following diafiltration with water (W, dotted line) or phosphate (P, dashed line) shown as references.

Table 1. pH, TS concentration, micelle size (hydrodynamic diameter), and phosphate (P) and calcium (Ca) concentrations of the final retentate following skim milk microfiltration and diafiltration (MF/DF)[1]

		Diafiltration solution[2]					
Parameter	Skim milk	DF-W	DF-P	DF-(P+Ca)	DF-Cit	DF-(Cit+Ca)	DF-(P+Cit+Ca)
pH	6.55 ± 0.01^{d}	7.02 ± 0.01^{b}	7.00 ± 0.01^{b}	6.22 ± 0.04^{e}	7.88 ± 0.01^{a}	6.98 ± 0.01^{b}	6.83 ± 0.04^{c}
TS (% wt/wt)	9.11 ± 0.05^{a}	6.93 ± 0.05^{g}	7.71 ± 0.02^{f}	8.88 ± 0.04^{b}	7.97 ± 0.01^{e}	8.31 ± 0.03^{d}	8.62 ± 0.04^{c}
Hydrodynamic diameter (nm)	167 ± 2^{b}	157 ± 4^{cd}	147 ± 4^{e}	150.8 ± 0.2^{de}	$174 \pm 10^{a,3}$ 23 ± 4^{f}	157 ± 1^{cd}	161 ± 2^{bc}
P (m*M*)	33 ± 3^{e}	38.5 ± 0.1^{d}	60.6 ± 0.1^{c}	94 ± 2^{a}	22.7 ± 0.2^{f}	40.6 ± 0.1^{d}	67 ± 5^{b}
Ca (m*M*)	32 ± 3^{e}	47.5 ± 0.2^{d}	48.5 ± 0.1^{d}	103 ± 2^{a}	19.3 ± 0.4^{f}	64.9 ± 0.2^{c}	70 ± 5^{b}

[a–g]Means within a row not sharing a common superscript letter are different ($P < 0.05$).

[1]Republished from Boiani et al. (2017).

[2]DF-W = DF with water; DF-P = DF with phosphate; DF-(P+Ca) = DF with a combined solution of phosphate and calcium; DF-Cit = DF with citrate; DF-(Cit+Ca) = DF with a combined solution of citrate and calcium; DF-(P+Cit+Ca) = DF with a combined solution of phosphate, calcium, and citrate.

[3]Citrate diafiltration destabilizes casein micelle structure, generating a binomial distribution. The smaller value is related to soluble casein, whereas the bigger value refers to casein that retains a structure similar to the casein micelle.

the FTIR spectrum of brushite was compared with ACP and dry or aqueous suspended CPN obtained by proteolytic digestion of CM (Lenton et al., 2016). The CPN spectra found in the Lenton et al. (2016) study consisted of a broad band falling within the same area as that of the brushite spectrum. A high-intensity band was observed at a lower wavenumber when CPN was suspended in water or deuterated water. However, the Lenton et al. (2016) study did not investigate CPN in milk or in casein suspensions. With respect to milk FTIR spectra, the present study uniquely identified the coexistence of 2 different populations of phosphate: P_i in solution and phosphate in the CPN bound to CM. Using a simple deconvolution method already used for protein structure studies (Byler and Susi, 1986; Curley et al., 1998), we could distinguish between different species of phosphorus of milk. As shown in Figure 1a, the 1,076 cm^{-1} band associated with P_i overlapped with that of CPN already found by Lenton et al. (2015), and identified from our spectra as a broad band at 1,041 to 1,022 cm^{-1} (Figure 2b and 2d). This region of the spectrum changed upon addition of different minerals during DF processing. During DF-W (Figure 3), the band belonging to CPN (1,041–1,022 cm^{-1}) increased in wavenumber by shifting to 1,055 to 1,036 cm^{-1}. However, considering the difference between the spectra of milk (Figure 2a and 2c) and that of DF-W (Figure 3a) when using water and MF permeate as background, a degree of uncertainty remains as to a possible confounding effect of lactose interference rather than a change in CPN. Specifically, considering the difference in absorbance between skim milk spectra with water (Figure 2a) and MF permeate backgrounds (Figure 2c), respectively, ≈0.10 and ≈0.002 A (where A indicates absorbance), lactose (with its maximum band occurring at 1,040–1,060 cm^{-1}) is clearly a factor. In addition, the difference in position of CPN bands between skim milk (1,038–1,022 cm^{-1}) with MF permeate background (Figure 2d) and DF-W (1,055–1,036 cm^{-1}; Figure 3b) cannot simply be explained by the DF influence alone, thus posing a question regarding the extent of lactose permeation during processing. In this regard, we decided to rely on the effectiveness of MF and DF to permeate residual lactose levels from the retentates as much as possible to increase the certainty that the bands are associated with different phosphorus species. Retention of P_i following DF-W, first observed by us (Boiani et al., 2017) using ^{31}P NMR, was also evident as a peak on the FTIR spectrum at 1,082 cm^{-1}.

By changing the DF solutions, we could observe changes in the spectrum of the band relating to CPN as represented by a change in the milk mineral equilibrium. Therefore, when DF solutions included P_i (DF-P, DF-P+Ca, DF-P+Cit+Ca), we could observe an increased absorbance of the bands associated with P_i (Figure 4a and c). This maintenance of P_i in solution is in agreement with the results obtained from ^{31}P NMR (Boiani et al., 2017). Furthermore, a previous study showed that addition of orthophosphate and calcium to sodium caseinate leads to precipitation of CP_i when the concentration of P_i exceeds 100 m*M* (Thomar et al., 2016). Considering the high ionic concentrations in DF-P+Ca (Table 1), phosphate and calcium might have precipitated as CP_i in this retentate, resulting in an FTIR spectrum with a similar shape as that shown in Figure 1c, consisting of 3 sharper bands at 1,119, 1,078, and 1,034 cm^{-1}. Although the first and second bands overlapped with the already visible bands of P_i, the third was distinguishable from the CPN band because of its different shape. Therefore, this suggests

that the band at 1,034 cm^{-1} (Figure 4a) represents CP_i precipitation in the final retentate. On the other hand, where calcium chelation is concerned, a calcium chelating agent, by interacting with Ca^{2+}, reduces the stability of CPN and, consequently, leads to the solubilization of the nanocluster and destabilization of the CM structure. Solubilization of CPN occurring during DF-Cit (Figure 4b) is in agreement with the reduction of the CPN band intensity at 1,055 to 1,036 cm^{-1} and concurs with the results established using ^{31}P NMR (Boiani et al., 2017). A particular combination of ions (DF-P+Cit+Ca) succeeded in minimizing CPN solubilization based on NMR signal interpretation (Boiani et al., 2017) and supported by quantitative chemical analysis, as reflected by the relative increase in FTIR signal of CPN (1,042–1,037 cm^{-1}) relative to P_i (1,078 cm^{-1}; Figure 4c). The CPN broad band higher absorbance of DF-P+Cit+Ca compared with DF-W and DF-P confirmed that solubilization of CPN was reduced by this DF step. Hence, these results show that FTIR is capable of differentiating between CPN, CP_i, and P_i. In particular, it promises to be a useful tool for investigating the qualitative distribution and repartitioning of different species of phosphorus by observing the 3 sets of phosphate bands (1,076 cm^{-1} for P_i, 1,035–1,060 cm^{-1} for CPN, and 1,034 cm^{-1} for CP_i). These ATR-FTIR markers may be usefully combined with ^{31}P NMR spectroscopy, especially because the later technique cannot distinguish between CPN and CP_i. Thus, the combination of ATR-FTIR with ^{31}P NMR illustrates the potential of applying advanced analytical instrumentation to improve knowledge and understanding of the mineral equilibrium of milk and its derivatives. Furthermore, the practical application of such techniques lends itself to a greater understanding of molecular changes, such as those occurring within CPN of CM and the inorganic fraction of salts present in milk during processing. Such analytical techniques offer considerable diagnostic potential when troubleshooting processes and improving product functionality.

ACKNOWLEDGMENTS

The authors acknowledge funding support under the Irish Department of Agriculture Food Institution Research Measure (FIRM) for this study. Mattia Boiani was the recipient of a Walsh Fellowship funding award by Teagasc (Teagasc, Administrative Head Office, Carlow, Ireland).

REFERENCES

AOAC. 1990. Official Methods of Analysis. 15th ed. Association of Official Analytical Chemists, Arlington, VA.

Berzina-Cimdina, L., and N. Borodajenko. 2012. Research of calcium phosphates using Fourier transform infrared spectroscopy. InTech Open Access Publisher, Rijeka, Croatia.

Boiani, M., P. McLoughlin, M. A. Auty, R. J. FitzGerald, and P. M. Kelly. 2017. Effects of depleting ionic strength on ^{31}P nuclear magnetic resonance spectra of micellar casein during membrane separation and diafiltration of skim milk. J. Dairy Sci. 100:6949–6961.

Byler, D. M., and H. M. Farrell Jr. 1989. Infrared spectroscopic evidence for calcium ion interaction with carboxylate groups of casein. J. Dairy Sci. 72:1719–1723.

Byler, D. M., and H. Susi. 1986. Examination of the secondary structure of proteins by deconvolved FTIR spectra. Biopolymers 25:469–487.

Cross, K. J., N. L. Huq, J. E. Palamara, J. W. Perich, and E. C. Reynolds. 2005. Physicochemical characterization of casein phosphopeptide-amorphous calcium phosphate nanocomplexes. J. Biol. Chem. 280:15362–15369.

Curley, D. M., T. F. Kumosinski, J. J. Unruh, and H. M. Farrell Jr.. 1998. Changes in the secondary structure of bovine casein by Fourier transform infrared spectroscopy: Effects of calcium and temperature. J. Dairy Sci. 81:3154–3162.

De Kruif, C. G. 2014. The structure of casein micelles: A review of small-angle scattering data. J. Appl. Cryst. 47:1479–1489.

Fox, P. F., and A. Brodkorb. 2008. The casein micelle: Historical aspects, current concepts and significance. Int. Dairy J. 18:677–684.

Gaucheron, F. 2005. The minerals of milk. Reprod. Nutr. Dev. 45:473–483.

Gebhardt, R., N. Takeda, U. Kulozik, and W. Doster. 2011. Structure and stabilizing interactions of casein micelles probed by high-pressure light scattering and FTIR. J. Phys. Chem. B 115:2349–2359.

Grewal, M. K., J. Chandrapala, O. Donkor, V. Apostolopoulos, L. Stojanovska, and T. Vasiljevic. 2017. Fourier transform infrared spectroscopy analysis of physicochemical changes in UHT milk during accelerated storage. Int. Dairy J. 66:99–107.

Hirsch, A., I. Azuri, L. Addadi, S. Weiner, K. Yang, S. Curtarolo, and L. Kronik. 2014. Infrared absorption spectrum of brushite from first principles. Chem. Mater. 26:2934–2942.

Holt, C. 1992. Structure and stability of bovine casein micelles. Pages 63–151 in Advances in Protein Chemistry. Vol. 43. C. B. Anfinsen, F. M. Richards, J. T. Edsall, and D. S. Eisenberg, ed. Academic Press, San Diego, CA.

Holt, C. 2004. An equilibrium thermodynamic model of the sequestration of calcium phosphate by casein micelles and its application to the calculation of the partition of salts in milk. Eur. Biophys. J. 33:421–434.

Holt, C., C. G. de Kruif, R. Tuinier, and P. A. Timmins. 2003. Substructure of bovine casein micelles by small-angle X-ray and neutron scattering. Colloids Surf. A Physicochem. Eng. Asp. 213:275–284.

Holt, C., P. A. Timmins, N. Errington, and J. Leaver. 1998. A core-shell model of calcium phosphate nanoclusters stabilized by β-casein phosphopeptides, derived from sedimentation equilibrium and small-angle X-ray and neutron-scattering measurements. Eur. J. Biochem. 252:73–78.

Holt, C., N. M. Wahlgren, and T. Drakenberg. 1996. Ability of a beta-casein phosphopeptide to modulate the precipitation of calcium phosphate by forming amorphous dicalcium phosphate nanoclusters. Biochem. J. 314:1035–1039.

Horne, D. S. 2006. Casein micelle structure: Models and muddles. Curr. Opin. Colloid Interface Sci. 11:148–153.

Kher, A., P. Udabage, I. McKinnon, D. McNaughton, and M. A. Augustin. 2007. FTIR investigation of spray-dried milk protein concentrate powders. Vib. Spectrosc. 44:375–381.

Lenton, S., T. Nylander, C. Holt, L. Sawyer, M. Härtlein, H. Müller, and S. C. M. Teixeira. 2016. Structural studies of hydrated samples of amorphous calcium phosphate and phosphoprotein nanoclusters. Eur. Biophys. J. 45:405–412.

Lenton, S., T. Nylander, S. M. Teixeira, and C. Holt. 2015. A review of the biology of calcium phosphate sequestration with special reference to milk. Dairy Sci. Technol. 95:3–14.

Little, E. M., and C. Holt. 2004. An equilibrium thermodynamic model of the sequestration of calcium phosphate by casein phosphopeptides. Eur. Biophys. J. 33:435–447.

Mekmene, O., Y. Le Graët, and F. Gaucheron. 2009. A model for predicting salt equilibria in milk and mineral-enriched milks. Food Chem. 116:233–239.

Singh, H. 2007. Interactions of milk proteins during the manufacture of milk powders. Lait 87:413–423.

Singh, R. P., Y. D. Yeboah, E. R. Pambid, and P. Debayle. 1991. Stability constant of the calcium-citrate(3-) ion pair complex. J. Chem. Eng. Data 36:52–54.

Thomar, P., A. Gonzalez-Jordan, J. Dittmer, and T. Nicolai. 2016. Effect of orthophosphate and calcium on the self assembly of concentrated sodium caseinate solutions. Int. Dairy J. 84:1–8. https://doi.org/10.1016/j.idairyj.2016.08.010.

Trpkovska, M., B. Šoptrajanov, and P. Malkov. 1999. FTIR reinvestigation of the spectra of synthetic brushite and its partially deuterated analogues. J. Mol. Struct. 480:661–666.

Upreti, P., and L. E. Metzger. 2006. Utilization of Fourier transform infrared spectroscopy for measurement of organic phosphorus and bound calcium in Cheddar cheese. J. Dairy Sci. 89:1926–1937.

Zhou, Q., S.-Q. Sun, L. Yu, C.-H. Xu, I. Noda, and X.-R. Zhang. 2006. Sequential changes of main components in different kinds of milk powders using two-dimensional infrared correlation analysis. J. Mol. Struct. 799:77–84.